THE ROYAL SOCIETY

Global relationship between anatomical connectivity and activity propagation in the cerebral cortex

Rolf Kötter[1] **and Friedrich T. Sommer**[2]

[1]*C. & O. Vogt Brain Research Institute, Heinrich Heine University, D-40225 Düsseldorf, Germany (rk@hirn.uni-duesseldorf.de)*
[2]*Department of Neural Information Processing, University of Ulm, Oberer Eselsberg D-89069 Ulm, Germany (fritz@neuro.informatik.uni-ulm.de)*

Anatomical connectivity is a prerequisite for cooperative interactions between cortical areas, but it has yet to be demonstrated that association fibre networks determine the macroscopical flow of activity in the cerebral cortex. To test this notion, we constructed a large-scale model of cortical areas whose interconnections were based on published anatomical data from tracing studies. Using this model we simulated the propagation of activity in response to activation of individual cortical areas and compared the resulting topographic activation patterns to electrophysiological observations on the global spread of epileptic activity following intracortical stimulation. Here we show that a neural network with connectivity derived from experimental data reproduces cortical propagation of activity significantly better than networks with different types of neighbourhood-based connectivity or random connections. Our results indicate that association fibres and their relative connection strengths are useful predictors of global topographic activation patterns in the cerebral cortex. This global structure–function relationship may open a door to explicit interpretation of cortical activation data in terms of underlying anatomical connectivity.

Keywords: cat cerebral cortex; association fibres; functional connectivity; strychnine neuronography; structure–function relationship; computer model

1. INTRODUCTION

In vivo tracing of anatomical connectivity has revealed dense networks of association fibres in the mammalian cerebral cortex (for summaries see Felleman & Van Essen 1991; Scannell *et al.* 1995; Young 1993). Compared to local microcircuitry and extracortical loops, association fibres provide a fast and direct route of information transfer between cortical areas. It is likely, therefore, that functional interactions between cortical areas correspond with the structural organization of association fibre networks.

Computer models can provide a direct test of this hypothesis. In a previous study, we showed that a collation of data from tracing studies could be used to construct a network of cortical areas for simulation of activity spread in the cerebral cortex (Sommer & Kötter 1997). Here we extend this approach, and evaluate different assumptions about the routes of cortical activity spread. First, we show that activity propagation observed in an experimental model of epilepsy is poorly explained by a limited spread to monosynaptically connected target areas. Therefore, an iterative prescription is used to accommodate controlled propagation to successively connected cortical areas. Second, we assess the spread of activity in a neural network whose connectivity is derived from anatomical experiments by comparing it to electrophysiologically ascertained topographic activation patterns that were induced by stimulation of the corresponding cortical regions. The performance of this network model is compared to randomly connected networks and to systematically connected networks based on neighbourhood. Finally, the temporal development of topographic activation patterns is discussed. Our analysis provides evidence of a global structure–function relationship between anatomical connectivity and activity propagation in the cerebral cortex, which may help to explain topographic activation patterns in functional paradigms and may help to specify interventions intended to modify the spread of epileptic activity.

2. METHODS

(a) *Model of cortical areas*

We devised a minimal model of cortical areas, the same for all cortical areas in all simulations. The model prescribed that a cortical area j was active at the next time step $(\tau + 1)$ if the sum of its activating inputs exceeded a certain threshold Θ, i.e. $x(\tau + 1)_j = \mathrm{H}[\Sigma_{i=1}^{n}\, w_{ij}\, x(\tau)_i - \Theta]\ \forall j$, where $\mathrm{H}[x]$ is the Heaviside function, n equals the total number of areas, w_{ij} denotes the coupling strength from area i to j, and $x(\tau)_i$ is the activity of the respective afferent area. The coupling strength was aligned to the anatomical connection strength: $w_{ij} = \langle s_{ij} \rangle^{\gamma}$ for $s_{ij} \in \{0, \ldots, 3\}$ and $\gamma = 2$. Excitatory self-feedback w_{ij} had a fixed value of 10, based on rough estimates of the proportion of extrinsic to intrinsic axon terminals in cortical areas. Control of the threshold ensured that the activity in the network spread smoothly: $\Theta(\tau + 1) = \max\{\Theta : |x(\tau)| < |x(\tau + 1)| \leqslant \alpha\}$, where $|x(\tau)| = \Sigma_{i=1}^{n} x(\tau)_i$ and α set the maximal number of active areas.

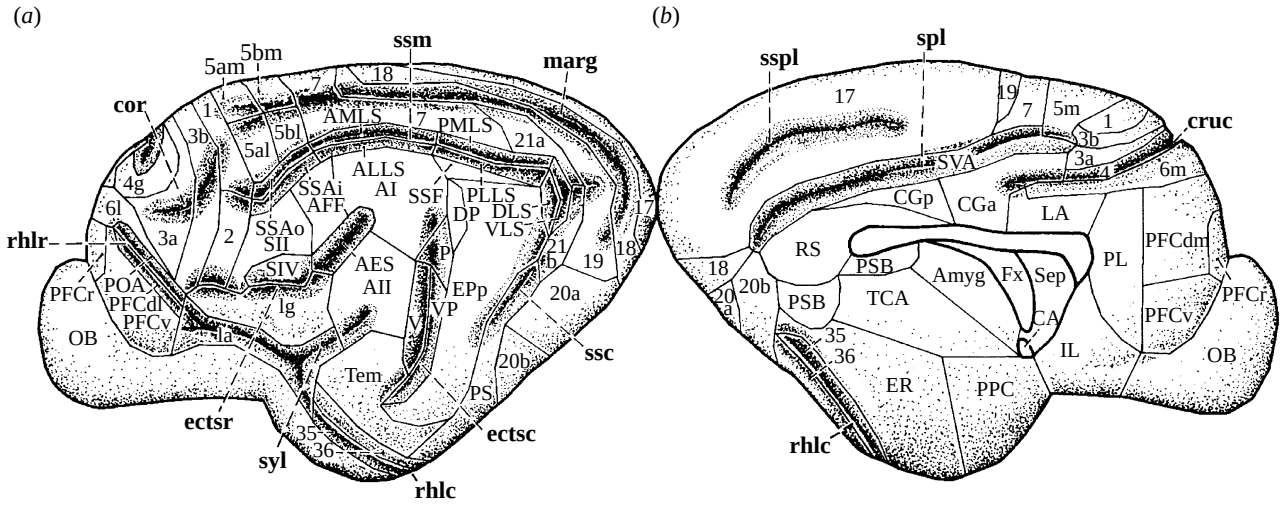

Figure 1. Map of the cerebral cortex of the cat showing the parcellation scheme used by Scannell *et al.* (1995) in a lateral view (*a*) and a medial view (*b*). The positions of areal borders are tentative. Areas referred to in this paper are: 20b, visual area on the posterior ectosylvian gyrus; 35, 36, areas of the perirhinal cortex; 7, multimodal sensory association area on the middle part of the suprasylvian gyrus; CGp, posterior part of cingulate cortex; EPp, a visual and auditory association area on the posterior part of the posterior ectosylvian gyrus; ER, entorhinal cortex; Ia, agranular insula; Ig, granular insula; IL, infralimbic area; LA, anterior limbic cortex; PFCdm, dorsomedial prefrontal cortex; PFCr, rostral prefrontal cortex; PSb, pre-, para-, and postsubicular cortex; SVA, splenial visual area; Tem, temporal auditory field. Abbreviations of sulci are denoted in bold lower case: cor, coronal sulcus; cruc, cruciate sulcus; ectsc, caudal ectosylvian sulcus; ectsr, rostral ectosylvian sulcus; marg, marginal sulcus; rhlc, caudal rhinal sulcus; rhlr, rostral rhinal sulcus; spl, splenial sulcus; ssc, caudal suprasylvian sulcus; ssm, medial suprasylvian sulcus; sspl, supraplenial sulcus; syl, sylvian sulcus.

(b) *Connectivity models*

To evaluate the influence of various types of connectivity on the spread of activity, we embedded the area model in a network of either experimentally derived or neighbourhood-based or random connectivity patterns. Experimental data were taken from the most recent collation of published association fibres in the cerebral cortex of the cat (Scannell *et al.* 1995). This collation contained 1139 reported corticocortical connections between 65 areas. In addition, it provided an estimate of anatomical connection strength for each projection. This experimentally derived connectivity model was compared to two neighbourhood-based connectivity models: the nearest-neighbour model linked only areas that had a common border, whereas the nearest-and-next-neighbour model additionally connected those areas that were, at most, one interposed area apart. Such neighbourhood-based patterns of connectivity could be relevant if activity propagated predominantly by local micro-circuitry in the cortical grey matter. The strengths of the neighbourhood-based connections were modelled by binary values ($w_{ij} \in \{0,1\}$) since empirical data of such connections were lacking. The performance of all three connectivity models was compared to chance results obtained with random connectivities of corresponding densities and strengths between the 65 areas. This allowed us to assess the predictive value of the experimentally derived and neighbourhood-based connectivity models.

(c) *Topographic activation patterns*

The network of 65 area models was wired according to each of the different connectivity schemes and the activation pattern was observed that occurred during continuous activation of a single area. We performed 14 such activations where the activated areas matched the ones stimulated in a study of strychnine neuronography in the cat cerebral cortex (figs 1B–6B in MacLean & Pribram (1953)). Experimental stimulations were carried out by local application of strychnine, an *in vivo* model of epileptic activity spread in the cerebral cortex (Holmes 1994; Kehne *et al.* 1997; Rostock *et al.* 1997). Saturated strychnine solution affecting a small patch of cortex (2 mm × 3 mm) in 18 anaesthetized cats led to local disinhibition by blockade of glycine and $GABA_A$ receptors (Klee *et al.* 1992; Shirasaki *et al.* 1991; Takahashi *et al.* 1994). Subsequently, bipolar electrodes were used to probe for propagation of epileptiform activity in a large set of other cortical regions. For each of the stimulation sites the resulting steady-state activities were diagrammatically summarized by the original authors differentiating strong firing, barely detectable firing, no firing and variable results between animals (see figs 1–6 in MacLean & Pribram (1953)). From the diagrams and additional explanations in the text, we mapped the topographic information to the parcellation scheme provided by Scannell *et al.* (1995) and assigned to each area one of the following activity values: active (corresponding to strong or barely detectable firing), silent (no firing) or unknown (variable results or no information). Of the 15 experiments described the first could not be implemented since the stimulated area (anterior pyriform area, figure 1*a*) had no corresponding representation in the structural connectivity matrix of Scannell *et al.* (1995).

(d) *Statistical evaluation*

Comparison between experimentally observed activation patterns and the steady-state patterns produced by the simulated activity spread was performed in the following way. The error was calculated as the average of the percentage of areas that were active in the simulation but silent in the experiments over all experimentally inactive areas (add_perc), and of areas silent in the simulation but active in the experiments over all active areas (miss_perc). Activity states in areas with experimentally unknown activity were ignored. The add_perc and miss_perc values could be traded off by adjusting the maximal

Table 1. *Errors averaged across 14 simulations using different connectivity models, gradings of connection strengths and modes of activity propagation*

(Mean percentages and standard deviations of errors are given for simulations with each model ('real'). Values denoted 'random' were obtained in simulations with randomly reshuffled connection topographies, whereas all other parameters matched the 'real' situation. The last column gives the significance level for different mean errors between the 'real' and the 'random' topographies.)

	real		random		
model	mean	s.d.	mean	s.d.	p
experimentally derived iterative graded	18.2	11.5	42.1	7.1	0.000
experimentally derived iterative binary	26.9	13.7	38.1	5.8	0.012
experimentally derived monosynaptic	33.0	14.9	50.1	1.9	0.001
nearest-neighbour connectivity	20.4	14.1	39.7	4.1	0.000
nearest-and-next-neighbour connectivity	20.0	17.3	37.3	5.5	0.003

number of active areas (determined by the parameter α), which was the only free parameter in the simulations and which was adjusted individually for each experiment to minimize the error.

Errors were calculated for each of the three connectivity models (experimentally derived, nearest-neighbour, nearest-and-next-neighbour) in all 14 simulated experiments. In addition, a number of control calculations were performed. First, it had been assumed that strychnine neuronography reveals only monosynaptic but not transsynaptic connectivity (Dusser de Barenne & McCulloch 1939; Frankenhaeuser 1951; MacLean & Pribram 1953). If this were true then our iterative prescription of activity propagation would be expected to produce more errors than simple activation of the immediate targets of the stimulated area. Second, Young *et al.* (1994) were interested in the robustness of topological analyses against errors in estimates of connection strengths. We made an analogous test of whether the connectivity model based on traced connectivity explained activity spread differently when tracing data determined the connectivity model but the connections strengths were binarized such that $w_{ij} \in \{0,1\}$. These five conditions were compared by analysis of variance for general multifactorial data (SPSS, v. 7.5, SPSS, Inc.). The connectivity model was regarded as a fixed factor for pairwise comparisons of main effects.

Finally, we controlled all simulations for chance results. To this end, we simulated for each connectivity model 20 controls with random connection topographies of corresponding density and grading. In the case of the monosynaptic activity spread 20 random activation patterns were generated that comprised the same number of active areas as prescribed by the monosynaptic projections from the stimulated area. Mean errors obtained with 'real' and 'random' topographies were assessed by t-tests for equal or unequal variances depending on the outcome of an f-test (Numerical Recipes Software). The differences between errors of the 'random' simulations and errors of the corresponding 'real' simulations were calculated so that positive values denoted a better than chance behaviour of the 'real' model. These data were analysed by a repeated measure analysis of variance (five groups, 14 experiments, 20 repetitions) with all other procedures as described above for multifactorial data.

Beyond static activation patterns, simulations of activity spread permitted inspection of the cortical routes taken during the development of the activity patterns. Successive steps of the developing activation patterns were displayed on maps of the cat cerebral cortex by use of the Mathematica software (Wolfram Research, Inc.) after modification of its WorldPlot package.

3. RESULTS

Table 1 shows that simulations based on the experimentally derived connectivity model with graded connection strengths using the iterative procedure to propagate activity in the network produced the smallest number of errors on average ($E_{\text{real}} = 18.2\%$). These were closely followed by the neighbourhood-based connectivity models, whereas binarizing connection strengths or limiting activity spread to one synapse degraded the performance considerably. Monosynaptic propagation of activity in the experimentally derived model had the highest average error ($E_{\text{real}} = 33.0\%$). Standard deviations obtained with all models were large, however, so that these simple statistics did not suffice to specify differences between the models.

Figure 2 gives a more detailed description of the differences between the three experimentally derived connectivity models across the 14 simulated experiments. It shows that, although the variation of errors between experiments with different stimulated areas was large, the three error curves had similar shapes. This indicates that there may be significant differences between the three models if the influence of the stimulated area was controlled for.

Analysis of variance confirmed the existence of significant differences ($p < 0.05$ across all five models). Pairwise comparisons (table 2, 'real') specified that simulating monosynaptic activity propagation in the experimentally derived connectivity model produced significant differences to all other models except the experimentally derived binary iterative model. The other four models including the binary iterative model could not be differentiated on this basis.

Having shown that the assumption of monosynaptic activity spread produced significantly more errors in the simulations than an iterative spread to secondary cortical areas, we examined whether any influence of the type of connectivity models could be demonstrated between the simulations. The key to this problem was to answer another question first: what percentage of errors obtained with each model was due to the specific topography of the connections as opposed to other possible influences such as their different densities or grading? We obtained an answer by shuffling the connections and by repeating the

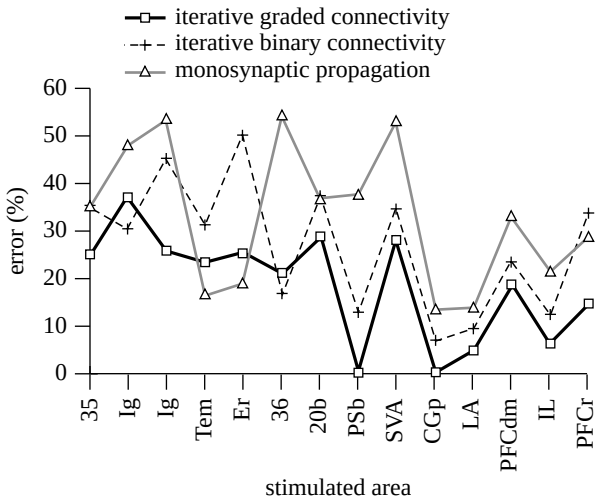

Figure 2. Influence of connection strengths (graded versus binary) and mode of activity propagation (iterative versus monosynaptic) on errors obtained in simulations of cortical activity spread using only connectivity models based on tracing data. Iterative graded, graded connection strengths and iterative activity propagation; iterative binary, binary connection strengths and iterative activity propagation; monosynaptic, activity propagation limited to immediate target areas. For abbreviations of stimulated areas see figure 1. Lines are added to emphasize the parallel course of errors obtained with the three models and do not indicate interpolation between experiments.

simulations with 20 such random connection topographies for each model.

Random topographies produced larger mean errors in replicating the electrophysiological experiments than the 'real' topographies, but had smaller standard deviations, due to the 20 repetitions (table 1, 'random'). Each pair of 'real' and 'random' topographies showed significantly different mean errors. The significance level was lowest for the experimentally derived binary model and highest for the experimentally derived, iterative graded and the nearest-neighbour model (table 1, 'p'). Figure 3 specifies the relationship between 'real' and 'random' for each experiment using the experimentally derived iterative graded connectivity model. Neither experimentally derived nor neighbourhood-based connectivities differed significantly from random connectivity on every single occasion. However, the experimentally derived, iterative graded model showed a consistent performance across all experiments, whereas the neighbourhood-based connectivity models and the experimentally derived iterative binary model performed better in some experiments and in others worse than their 'random' counterparts.

Subtracting errors obtained with 'real' connectivity from errors obtained with corresponding 'random' connectivities allowed us to quantify the difference from random in each of 20 repetitions of 14 experiments with five models. These differences were subjected to a repeated-measure analysis of variance, which showed that the differences between the five models were highly significant ($p < 0.001$). Again, we performed pairwise comparisons and obtained the clear-cut result (table 2, 'random minus real') that the experimentally derived iterative graded and binary models differed with high

Table 2. *Significance of differences in pairwise comparisons between five models*

(The models were: 1, experimentally derived iterative graded; 2, experimentally derived iterative binary; 3, experimentally derived monosynaptic; 4, nearest-neighbour connectivity; 5, nearest-and-next-neighbour connectivity. Values were obtained by analysis of variance and main model effects under two conditions: errors on simulating the 'real' model (left), and difference between errors simulating the 'real' and the randomly reshuffled models (right).)

	real				random minus real			
model	1	2	3	4	1	2	3	4
2	0.116	—	—	—	0.000	—	—	—
3	0.008	0.263	—	—	0.000	0.000	—	—
4	0.688	0.239	0.024	—	0.000	0.000	0.059	—
5	0.733	0.216	0.020	0.952	0.000	0.000	0.891	0.080

significance from each other and all other models. By contrast, the two neighbourhood-based and the experimentally derived monosynaptic models were indistinguishable in terms of their differences from random networks. This distinction could be illustrated by plotting the cumulative error reduction (i.e. the sums of the differences between 'random' and 'real') along the 14 experiments (figure 4). The small error differences between the models in each experiment summed up to differentiate—as the most superior—the experimentally derived iterative graded connectivity model from the group of neighbourhood-based connectivity models. The latters' performance was very similar to the experimentally derived model with monosynaptic activity propagation. The experimentally derived iterative binary model showed the smallest overall improvement compared to random connectivity, and was worse even than random networks in a few experiments.

4. DISCUSSION

This simulation approach to exploring structure–function relationships provides direct tests of the hypothesis that experimentally demonstrated structural connectivity is an important determinant of the spread of cortical activity. To minimize confusion with other influences, we took care to create an extremely simple model of cortex and cortical interactions using the same area model in every case. Clearly, this simplification does not match reality, and we have no reason to believe that the fine structure of cortical areas can be ignored. The challenge was not, however, to create a network sufficiently complex that it could be tuned to perfectly match the topography of activation patterns. Rather, we wanted to devise a strong test of the importance of knowledge about the structural connectivity between cortical areas to predict the spread of cortical activity. From this point of view, the simplicity of the model was a necessity to gain results whose validity was not diminished by uncontrolled influences of other factors.

The different mean errors obtained with the same experimentally derived model simulating monosynaptic

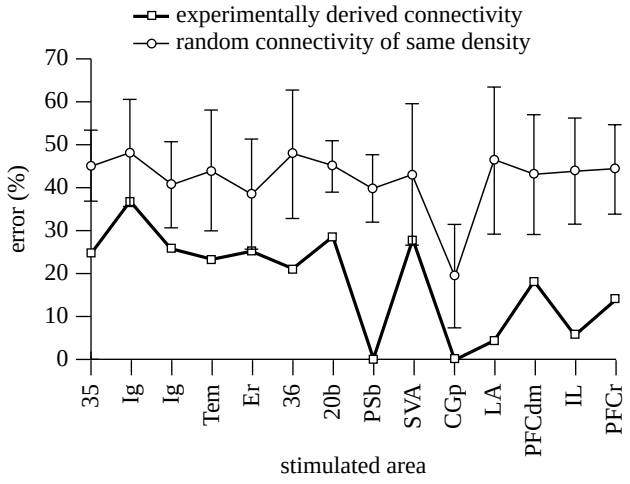

Figure 3. Errors obtained in simulations of cortical activity spread using the experimentally derived iterative graded connectivity model and 20 models with random connectivities of the same density and grading (mean ± s.d.). Lines between experiments are added for clarity and do not indicate interpolation.

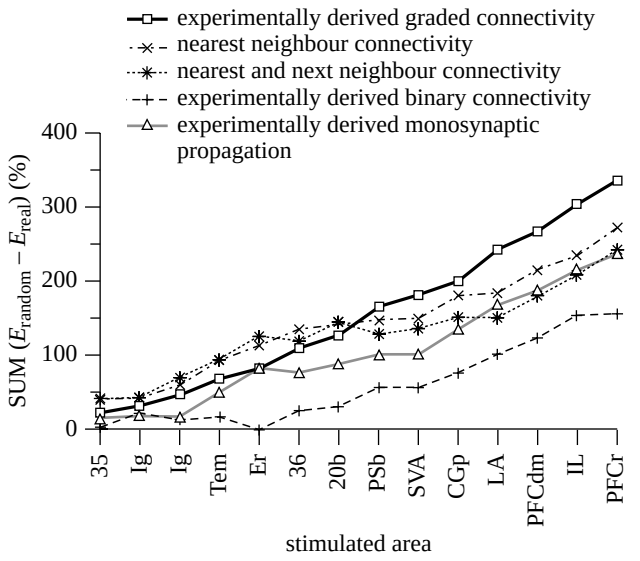

Figure 4. Cumulative differences between errors obtained with corresponding 'random' and 'real' connectivity models over 14 experiments. Note that the cumulative error difference decreases if the 'real' connectivity model performs worse than 'random'. Lines are added to aid recognition of the five models and do not indicate interpolation.

versus iterative activity propagation argue strongly against the assumption that strychnine neuronography demonstrated only monosynaptic projections between cortical areas. Although mean error is a useful measure to compare different simulation procedures for the same network model, comparisons of performance between different network models are complicated by the remaining differences in connection density and grading of connection strength. Thus, the specific reduction of error between each 'real' model and the corresponding 'random' model provides a better assessment of the specific influences of different density and grading. Here the experimentally derived graded model performed far better than the other models. Compared to the neighbourhood-based connectivity models this clear superiority was not completely expected since: (i) some activity spread might have occurred by contiguity of the grey matter between neighbouring areas; and (ii) there is a substantial overlap between experimentally derived and neighbourhood-based connectivity. Scannell *et al.* (1995), for example, calculated that the nearest-neighbour model comprised 25.8% of experimentally reported connections, and the nearest-and-next-neighbour model 56.0%. On the other hand, 69.0% of connections in the nearest-neighbour model were covered by the experimental data, but only 48.5% of connections in the nearest-and-next-neighbour model. Thus, despite a substantial overlap between experimentally derived connectivity and neighbourhood-based connectivities the remaining connectivity mismatches made a clear difference in performance. Compared to the experimentally derived binary model, the grading of connection strengths produced a far better performance. In contrast, Young *et al.* (1994) found that graded and binary connectivity matrices produced similar configurations in their structural analyses. However, the similar shape of the error curves across the 14 experiments (figure 2) confirmed that the two models were quite different as regards accounting for activity spread. Several explanations for this apparent mismatch may be considered. First, it is possible that values of weak connection strengths in the anatomical data may contain false positives, not always distinguishable from background labelling (Scannell 1995). Since in our binary grading, values of weak connection strength were credited with the same status as strong connection strengths, such a problem would have increased the noise and thereby decreased the performance of the model (Scannell 1995). Second, the effects of existing and absent connections on the results of topological analyses are of a very different nature than their influences on an iterative procedure for spreading simulated activity through a network.

Having demonstrated a link between detailed anatomical studies and the spread of activation, it is useful to consider possible reasons for the remaining mismatches between our simulations and the experiments. One reason for mismatches is a lack of precision in the underlying data: the structural information available from experiments and collated by Scannell *et al.* (1995) was certainly incomplete (see Scannell *et al.*, this issue; Hilgetag & Grant, this issue). For example, the allocortical regions of the cortex were not represented in detail and some areas (prepiriform cortex, corticoamygdaloid transition area, olfactory bulb) were omitted. Nevertheless, the global analyses of cortical network connectivity in the cat by Hilgetag, Burns, O'Neill, Scannell & Young (this issue) indicate that the available data characterize an efficiently structured network with dense clusters and comparatively short path lengths (Watts & Strogatz 1998). The electrophysiological data we have used here were even more limited. Although there are a few more studies of strychnine-induced activity spread in the cerebral cortex of the cat (e.g. Garol 1942*a*,*b*) we limited our investigation to one article (MacLean & Pribram 1953), for the reason that it presented a homogeneous set of experiments that were

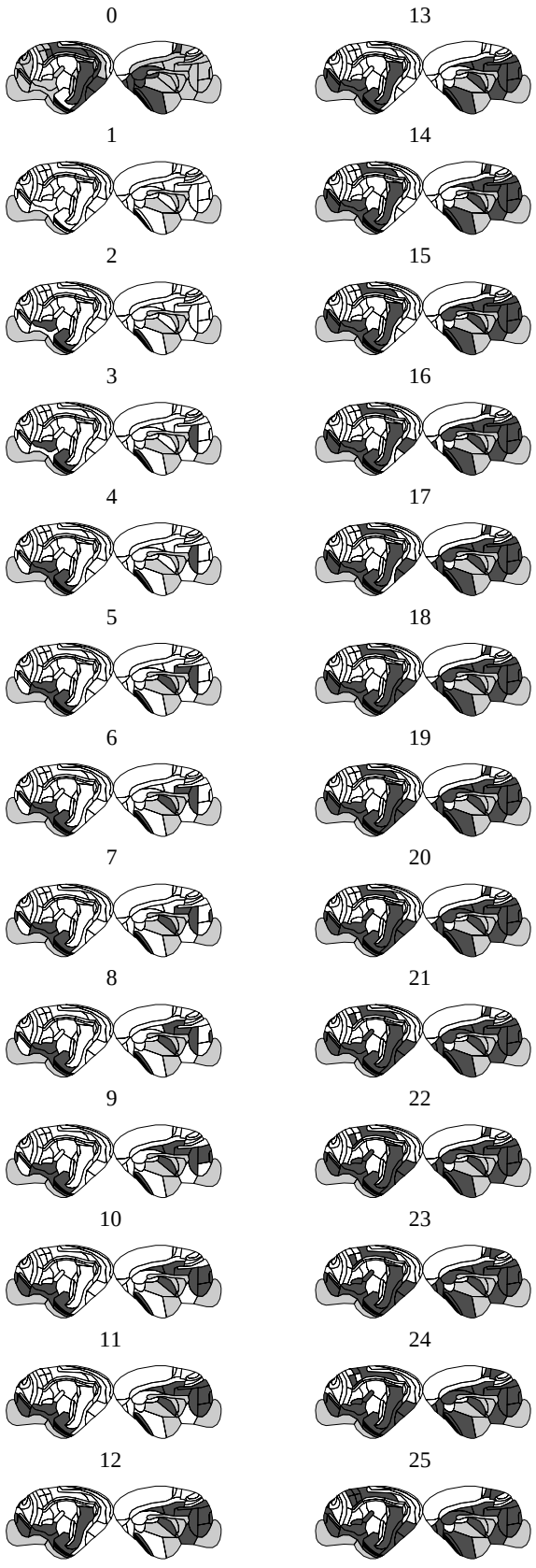

Figure 5. Successive steps of simulated activity propagation in the experimentally derived iterative graded model of the cat cerebral cortex. 0, the experimentally observed activation pattern as described by Pribram & MacLean (1953, their fig. 2B). The stimulated part of the fusiform gyrus is black, active areas are dark grey, inactive areas are white, areas of unknown activity are light grey. 1, the simulation started with stimulation (black area) of area 36 in the perirhinal cortex. 2–11, simulated activity (dark grey) spread to most ventral and frontomesial areas. 12–25, following activation of areas EPp and 7 in the parietal cortex, the activity on the lateral cortical surface spread rostrally to all subareas of area 5.

relatively comprehensive and well documented. A global network characterization of the functional matrix by means of cluster coefficients and path lengths was not helpful, since the limitation to 14 stimulation experiments defined several separate small clusters with few feedback connections. Where global network analyses fail, a simulation approach can still provide useful insights, as we hope we have shown. A major source of uncertainty was the topographic mapping between structural and functional data. Both Scannell *et al.* (1995) and MacLean & Pribram (1953) presented schematic lateral and medial views of the feline cerebral cortex that permitted a mapping only by reference to gross landmarks such as the larger sulci. Regions with strong curvatures (insula, ventral parts of frontal and temporal regions) could be attributed between maps only with considerable uncertainty. These problems are reduced where more extensive and more detailed data are available, as for strychnine neuronography in the macaque monkey (see Stephan, Hilgetag, Burns, O'Neill, Young & Kötter, this issue) and when more rigorous procedures for relating different parcellation schemes can be applied (see Stephan, Zilles & Kötter, this issue).

Another reason for mismatches was the simplicity of the model, which precluded error-free reproduction of activation patterns. In a few experiments, the spread of activity passed through an error-free pattern and settled into a different final state. Thus, even if the model had a path from the initial stimulation to a correct state, the experimentally observed activation patterns were not necessarily fixed point attractors of the simulated network. From the initial basis of our study, however, further hypotheses about factors influencing the topographic activity patterns can be tested in the future. Among these could be differential conduction velocities between pathways, differences in area interactions related to forward and backward connections between cortical areas, and different intrinsic processing in granular and agranular areas. As with other neuroinformatic studies (e.g. Hilgetag *et al.* 1996; Jouve *et al.* 1998; Young 1993; Young *et al.* 1994) we could prepare a list indicating what coupling strength presently unknown pathways should have in order to minimize the mismatch, suggesting further experiments.

Although every final topographic activation pattern resulting from the 14 simulations of the experimentally derived iterative graded model was different, many of them shared some constant features. The regions activated usually comprised ventrolateral regions including insular and perirhinal cortex, and frontomesial regions including cingulate cortex, areas LA, PL and medial prefrontal cortex (e.g. figure 5). Two other commonly activated areas were the posterior ectosylvian gyrus and area 7, which are both known to respond experimentally to stimuli in more than one sensory modality. The frequent activation of these areas was

related to the selection of stimulation sites surrounding the hilus of the hemispheres. Indeed, MacLean & Pribram (1953) designed their study to find evidence for mutual activation among these areas and regarded this evidence as a defining criterion of a 'limbic system'. Furthermore, they considered their findings to be a strong argument for a strategic role of 'limbic' cortex in cortical information processing. Thus, both structural and functional data point to sets of strongly interacting areas in ventral and frontomesial cortical regions, and to dense connectivity along the suprasylvian gyrus in the caudorostral direction. This correspondence between structurally and functionally defined sets of cortical areas, however, is not sufficient to characterize either a cortical 'system' or its 'limbicness' (Kötter & Meyer 1992; Kötter & Stephan 1997; Hilgetag, Burns, O'Neill, Scannell & Young, this issue).

Our computer simulations have another benefit compared to static analyses of structural connectivity, such as non-metric multidimensional scaling (Young *et al.* 1995), optimal set analysis (Hilgetag *et al.*, this issue) or structural equation modelling of more dynamic data (Büchel & Friston 1997; McIntosh & Gonzalez-Lima 1994): this is the explicit consideration of time. A striking observation during these simulations was the selective propagation of activity to the suprasylvian gyrus (figure 5), a pattern that was observed by MacLean & Pribram (1953), and which contradicts activity spread by mere neighbourhood. Even more interesting is the temporal sequence of this pattern, starting in area 7 in the posterior parietal cortex and propagating rostrally to all parts of area 5. When screening the literature for this peculiar observation we were astounded to see that Amzica & Steriade (1995) had described the clear preference of this posterior-to-anterior spread of activity in intra- and extracellular paired recordings from anterior and posterior regions of the suprasylvian gyrus (see fig. 2 in Amzica & Steriade (1995)). Further examples of our simulations are available at (http://www.hirn.uni-duesseldorf.de/∼rk/cx/catnetwork/sims.htm).

The present simulations point to the relevance of anatomical tracing studies for the explanation of the propagation of cortical activity. Clearly, this study is limited to the propagation of epileptiform activity, which, because of its intensity, may be more strictly defined by the global topography of the anatomical network than meaningful physiological activity during specific information processing tasks. However, simulations based on association fibre connectivity have potential for investigating effects of pharmacological and surgical procedures on the topographic spread of epileptic activity. A next step would be to evaluate activation of cerebral cortical areas during different behavioural situations as, for example, determined by 2-deoxyglucose mapping in the cat (Vanduffel *et al.* 1995, 1997). Considering primate brains, it would be interesting to investigate the use of our approach for interpreting activation patterns observed in functional imaging studies. This approach could thus complement the strategies pursued by structural equation modelling of functional connectivity, which have been based on guessed neuroanatomical connections (see, for example, Büchel & Friston 1997; McIntosh & Gonzalez-Lima 1994).

We thank Axel Schleicher for excellent statistical support and Claus C. Hilgetag for calculation of network coefficients. Malcolm P. Young, Jack W. Scannell and Klaas E. Stephan provided helpful comments on the manuscript and Christine Opfermann-Rüngeler embellished figure 1.

REFERENCES

Amzica, F. & Steriade, M. 1995 Disconnection of intracortical synaptic linkages disrupts synchronization of a slow oscillation. *J. Neurosci.* **15**, 4658–4677.

Büchel, C. & Friston, K. J. 1997 Modulation of connectivity in visual pathways by attention: cortical interactions evaluated with structural equation modelling and fMRI. *Cerebr. Cortex* **7**, 768–778.

Dusser de Barenne, J. G. & McCulloch, W. S. 1939 Physiological delimitation of neurones in the central nervous system. *Am. J. Neurophysiol.* **127**, 621–628.

Felleman, D. J. & Van Essen, D. C. 1991 Distributed hierarchical processing in the primate cerebral cortex. *Cerebr. Cortex* **1**, 1–47.

Frankenhaeuser, B. 1951 Limitations of method of strychnine neuronography. *J. Neurophysiol.* **14**, 73–79.

Garol, H. W. 1942*a* The 'motor' cortex of the cat. *J. Neuropath. Exp. Neurol.* **1**, 139–145.

Garol, H. W. 1942*b* The functional organization of the sensory cortex of the cat. II. *J. Neuropath. Exp. Neurol.* **1**, 320–329.

Hilgetag, C.-C., O'Neill, M. A. & Young, M. P. 1986 Indeterminate organization of the visual system. *Science* **271**, 776–777.

Holmes, O. 1994 The intracortical neuronal connectivity subserving focal epileptiform activity in rat neocortex. *Exp. Physiol.* **79**, 705–721.

Jouve, B., Rosenstiehl, P. & Imbert, M. 1998 A mathematical approach to the connectivity between the cortical visual areas of the macaque monkey. *Cerebr. Cortex.* **8**, 28–39.

Kehne, J. H., Kane, J. M., Chaney, S. F., Hurst, G., McCloskey, T. C., Petty, M. A., Senyah, Y., Wolf, H. H., Zobrist, R. & White, H. S. 1997 Preclinical characterization of MDL 27,192 as a potential broad spectrum anticonvulsant agent with neuroprotective properties. *Epilepsy Res.* **27**, 41–54.

Klee, M. R., Shirasaki, T., Nakaye, T., Akaike, N. & Melikov, E. N. 1992 Interaction of strychnine and bicuculline with GABA- and glycine-induced chloride currents in isolated CA1 neurons. In *Epilepsy and inhibition* (ed. E. J. Speckmann & M. J. Gutnick), pp. 93–106. München, Germany: Urban & Schwarzenberg.

Kötter, R. & Meyer, N. 1992 The limbic system: a review of its empirical foundation. *Behav. Brain Res.* **52**, 105–127.

Kötter, R. & Stephan, K. E. 1997 Useless or helpful? The 'limbic system' concept. *Rev. Neurosci.* **8**, 139–146.

McIntosh, A. R. & Gonzalez-Lima, F. 1994 Structural equation modeling and its application to network analysis in functional brain imaging. *Hum. Brain Mapp.* **2**, 2–22.

MacLean, P. D. & Pribram, K. H. 1953 Neuronographic analysis of medial and basal cerebral cortex. I. Cat. *J. Neurophysiol.* **16**, 312–323.

Rostock, A., Tober, C., Rundfeldt, C., Bartsch, R., Unverferth, K., Engel, J., Wolf, H. H. & White, H. S. 1997 AWD 140–190: a new anticonvulsant with a very good margin of safety. *Epilepsy Res.* **28**, 17–28.

Scannell, J. W. 1995 The connectional organization of the cat cerebral cortex. DPhil thesis, University of Oxford, UK.

Scannell, J. W., Blakemore, C. & Young, M. P. 1995 Analysis of connectivity in the cat cerebral cortex. *J. Neurosci.* **15**, 1463–1483.

Shirasaki, T., Klee, M. R., Nakaye, T. & Akaike, N. 1991 Differential blockade of bicuculline and strychnine on

GABA- and glycine-induced responses in dissociated rat hippocampal pyramidal cells. *Brain Res.* **561**, 77–83.

Sommer, F. T. & Kötter, R. 1997 Simulating a network of cortical areas using anatomical connection data in the cat. In *Computational neuroscience. Trends in research* (ed. J. M. Bower), pp. 511–517. New York: Plenum.

Takahashi, Y., Shirasaki, T., Yamanaka, H., Ishibashi, H. & Akaike, N. 1994 Physiological roles of glycine and gamma-aminobutyric acid in dissociated neurons of rat visual cortex. *Brain Res.* **640**, 229–235.

Vanduffel, W., Vandenbussche, E., Singer, W. & Orban, G. A. 1995 Metabolic mapping of visual areas in the behaving cat: a [^{14}C]2-deoxyglucose study. *J. Comp. Neurol.* **354**, 161–180.

Vanduffel, W., Vandenbussche, E., Singer, W. & Orban, G. A. 1997 A metabolic mapping study of orientation discrimination and detection tasks in the cat. *Eur. J. Neurosci.* **9**, 1314–1328.

Watts, D. J. & Strogatz, S. H. 1998 Collective dynamics of 'small-world' networks. *Nature* **393**, 440–442.

Young, M. P. 1993 The organization of neural systems in the primate cerebral cortex. *Proc. R. Soc. Lond.* B **252**, 13–18.

Young, M. P., Scannell, J. W., Burns, G. A. P. C. & Blakemore, C. 1994 Analysis of connectivity: neural systems in the cerebral cortex. *Rev. Neurosci.* **5**, 227–249.

Young, M. P., Scannell, J. W., O'Neill, M. A., Hilgetag, C. C., Burns, G. & Blakemore, C. 1995 Non-metric multidimensional scaling in the analysis of neuroanatomical connection data and the organization of the primate cortical visual system. *Phil. Trans. R. Soc. Lond.* B **348**, 281–308.